# Journal Pre-proof

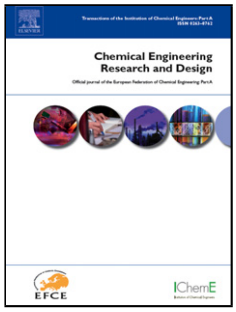


The effect of energy recovery device and feed flow rate on the energy efficiency of reverse osmosis process

Adnan Alhathal Alanezi Ali Altaee Adel O. Sharif

PII: S0263-8762(20)30120-9

DOI: https://doi.org/doi:10.1016/j.cherd.2020.03.018

Reference: CHERD 4038

To appear in: *Chemical Engineering Research and Design*

Received Date: 8 February 2020

Accepted Date: 12 March 2020

Please cite this article as: Alanezi, A.A., Altaee, A., Sharif, A.O.,The effect of energy recovery device and feed flow rate on the energy efficiency of reverse osmosis process, *Chemical Engineering Research and Design* (2020), doi: https://doi.org/10.1016/j.cherd.2020.03.018

# The effect of energy recovery device and feed flow rate on the energy efficiency of reverse osmosis process

**Adnan Alhathal Alanezi[1*], Ali Altaee[2], Adel O. Sharif[3]**

[1]Department of Chemical Engineering Technology, College of Technological Studies, The Public Authority for Applied Education and Training (PAAET), P.O.BOX 42325, Shuwaikh 70654, Kuwait, E-mail: aa.alanezi@paaet.edu.kw

[2]School of Civil and Environmental Engineering, University of Technology Sydney, Ultimo, NSW 2007, Australia.

[3]Centre for Osmosis Research and Applications (CORA), Chemical and Process Engineering Department, Faculty of Engineering and Physical Sciences, University of Surrey, Guildford GU2 7XH, UK.

## Highlights:

1. Desalination power consumption of RO alone increased with increasing Re.
2. Power consumption was dependent on Re when pretreatment energy is added.
3. High pressure pump ($E_{pp}$) was responsible for 57-68% of total power consumption.
4. $E_{pp}$ was higher for RO with 95% ERD efficiency followed by 80% & 65% efficiency.

## Abstract

The energy requirements for reverse osmosis (RO) seawater desalination continue to be a major matter of debate. Previous studies have shown the dependence of optimum RO desalination energy on the RO recovery rate. However, they overlooked including the effect of Energy Recovery Device (ERD) and pretreatment on the power consumption. In this work, a computer model was used to analyze the energy requirements for RO desalination, taking into account the effect of ERD efficiencies and pretreatment. The specific power consumption (SPC) of the RO was found to increase with the increase of RO recovery rate when the ERD system was included. The optimum SPC became more dependent on the RO recovery rate when the pretreatment energy was added. The recovery for optimum desalination energy was 46%, 44%, and 40% for the RO system coupled with an ERD of 65%, 80%, and 95% efficiency, respectively. The results showed that RO process could be operated at lower recovery rate and still meet the projected desalination capacity by increasing the feed flow rate and coupling with high-efficiency ERD. A trivial decrease of the total desalination energy was achieved when the feed flow rate increased from 7 $m^3$/h to 8 $m^3$/h and recovery rate decreased from 46% to 44% by coupling the RO with an ERD of 95% efficiency. This suggests that the RO–ERD system can be operated at a high feed flow rate and low recovery rate without affecting the plant capacity.

Keywords: Reverse Osmosis; Desalination; Energy; Energy Recovery Device; Seawater; Specific Power Consumption

## 1. Introduction

Reverse Osmosis (RO) has been used successfully for seawater desalination for several decades to recover drinking water from seawater over a wide range of feed salinities [1-6]. Modern RO membranes typically exhibit greater than 99% rejection of monovalent ions and relatively high-water permeability, which makes them compatible with saline water treatment [7-8]. In comparison with the Multi-Stage Flash (MSF) and Multi-Effect Distillation (MED) technologies, the RO process is more energy efficient and provides higher water recovery rates [9]. MSF and MED recovery rates are *ca.* 30%, whereas RO recovery rates can reach 50% for 35 g/L salinity seawater. Commercial 8-inch (0.2 m) diameter RO membranes are characterized by a recovery rate between 10 and 30% per element; hence, several RO modules are packed in series inside each pressure vessel to achieve the desirable RO total

water recovery rate. Water permeation results in an increase of feed concentration from the lead to the tail RO element in the pressure vessel, whereas the recovery rate decreases. The flow rate of brine concentrate in the RO vessel should meet a certain minimum value to prevent RO fouling due to the precipitation of sparingly soluble salts [10].
Electricity requirements have often been cited as potential drawbacks for implementation of RO processes [9]. However, RO power consumption has been reduced since the invention of ERD [2, 11]. Without ERD, the energy requirement for desalinating seawater at standard salinity of 35 g/L is approximately 4 kWh/m$^3$ [2, 11-12]. With an ERD, the energy requirement for standard seawater desalination is about 2 kWh/m$^3$ [12, 13]. Hydraulic feed pressure is the main driving force for fresh water production from seawater in the RO process is responsible for most of the energy consumption [5]. However, minor energy consumption has incurred due to the pretreatment of seawater and should be added to the desalination power consumption [2, 14]. Karabelas and coworkers performed an energy analysis of a RO system using 40 g/L seawater salinity and an ERD efficiency of 95% [15]; 7 RO elements were packed in the pressure vessel system [15-17] and specific energy consumption was calculated. Their study showed that 50% of the SPC was due to the osmotic pressure of the seawater and incurred by the high-pressure pump. The impact of recovery rate on the performance of RO has been reported [16]; operation at a low recovery rate was found to decrease the membrane scale fouling because of the lower feed concentration to the RO membrane. As such, for a fixed permeate flow rate, the recovery rate of RO can be potentially decreased by increasing the feed flow rate.

Unfortunately, neither the impact of feed flow rate nor the efficiency of an ERD upon the SPC of multi-element RO systems has been investigated yet. Therefore, there is a gap in the general understanding of these aforementioned parameters on the power consumption of a RO system. Furthermore, the SPC of seawater pretreatment should be added to the SPC of the RO membrane since pretreatment is an essential stage in the RO process to avoid fouling of membranes and equipment [9, 14]. Therefore, the aim of this study was to calculate the SPC of a RO process at different feed flow rates for 65, 80, and 95% ERD efficiencies. The performance of seawater RO membrane system was investigated using a developed computer program which was validated with experimental data [17] and Reverse Osmosis System Analysis (ROSA 9.1) software. Outcomes of this study would be helpful in designing a RO–ERD system based on 8-inch RO modules. This study also provides an insight into the SPC and distribution in a multi-element pressure vessel.

## 2. Theoretical Background of RO-SPC

The SPC of a RO desalination process depends on a number of key operating and environmental parameters [5, 17]. The mathematical formula that has been suggested for calculating the SPC of the RO membrane without ERD system is as shown in equation 1 [5, 17]:

$$E_s = \frac{P_f * Q_f}{Q_p . \eta} \qquad [1]$$

where $E_s$ is the SPC for RO desalination (kWh/m$^3$); $P_f$ is the RO feed pressure (bar); $Q_f$ and $Q_p$ are the feed and permeate flow rates, respectively (m$^3$/h); $\eta$ is a constant representing the pump efficiency (0.8). Including the ERD system and adding the power consumption by the booster pump, the SPC of the RO membrane with ERD system $E_{s\text{-}RO}$ for desalination is calculated from equation 2:

$$E_{s-RO} = \frac{P_{pp} * Q_p + P_b * Q_c}{\eta * Q_p} \quad [2]$$

where $P_{pp}$ and $P_b$ are the pressure of high-pressure pump and booster pump (bar), respectively; $Q_c$ is the concentrate flow rate ($m^3$/h), which is equal to the difference between feed and permeate flow rates; this flow is recycled to the ERD system (figure 1). It was assumed that the efficiencies of the high-pressure pump and booster pump were equal to 0.8 [17]. Salt leakage in the ERD system has been detected and varied from one system to another [4]. Brine mixing with seawater, slightly, increases the salinity and osmotic pressure of feed solution in the RO stage [2]. The increase in feed salinity requires extra 2 bar feed pressure; equation (3) roughly estimates the increase in the seawater feed salinity, (SI) [2]:

$$SI = Re \times 6.15\% \quad [3]$$

where Re is the recovery rate of the RO system.

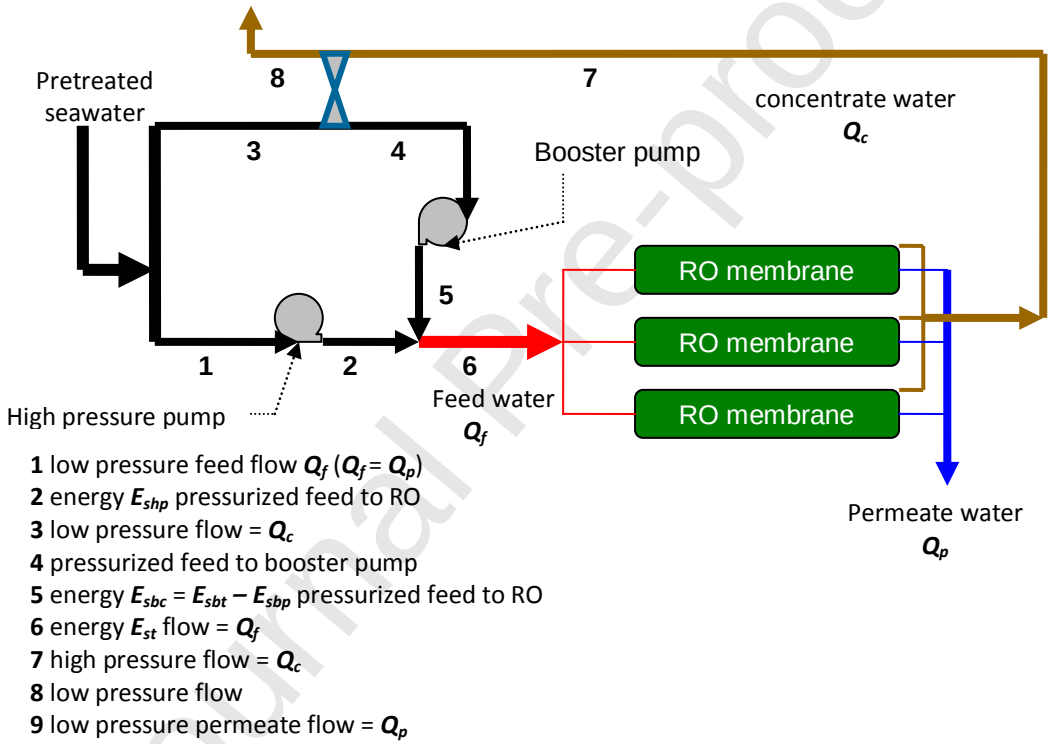


Figure 1: Schematic diagram of RO system with ERD

Pretreatment energy included the energy requirements for seawater pumping from the intake system, pretreatment energy, and supply pump energy. Additionally, energy for brine discharge should be included when the total desalination energy is calculated. As such, the total desalination energy included energies consumed by the high-pressure booster pumps, pretreatment energy, and brine discharge energy as in equations 4a & 4b:

$$E_{st} = \frac{P_{pp} * Q_p + P_b * Q_c + P_{pret} * Q_f + P_{dis} * Q_c}{\eta * Q_p} \quad [4a]$$

$$E_{st} = E_{pp} + E_{sb} + E_{spret} + E_{sdis} \quad [4b]$$

where $E_{st}$ is the total SPC of desalination (kWh/m$^3$); $E_{pp}$, $E_{sb}$, $E_{spret}$, and $E_{sdis}$ are the SPC of high-pressure pump, booster pump, pretreatment pumps, and brine discharge pump (kWh/m$^3$), respectively; $P_{pret}$ is the pressure required for seawater including intake, pretreatment, and supply pumps (bar); $P_{dis}$ is the pressure required for brine discharge (bar); $Q_f$ is the feed flow rate (m$^3$/h). The pressure required for seawater pretreatment was approximately estimated as follows: 4 bar for intake system; 2 bar for pretreatment supply pump; 4 bar for pretreatment process and supply pump to the RO system [2, 22]. Brine disposal required 2 bar for pumping and discharge to sea [22]. $E_{st}$ was analyzed here according to equation (4) taking into account the impact of feed flow rate. At fixed permeate flow rate, $E_{spret}$ and $E_{sdic}$ increase as the feed flow rate increases while the impact of $E_{pp}$ and $E_{sb}$ varies depending on the efficiency of ERD (figure 1).

## 3. Results and Discussion

### 3.1 Impact of ERD Efficiency

Applying equation (1) to calculate the SPC of RO showed that the minimum power consumption for 35 g/L seawater salinity occurred at 50% recovery rate (figure 1). These calculations were only valid for RO system without an ERD or without taking into account the energy requirements for pretreatment and brine discharge. The RO module SW30HRLE-440 was used in the simulation because of its high rejection rate to NaCl [16]. This result was in harmony with the view that optimum SPC for seawater desalination is directly related to the RO recovery rate [5, 19]. Previous studies have shown that the SPC of RO desalination tends to increase at low and high recovery rates but reaches an optimum amount in between as shown in figure 2 [5, 19]. Therefore, the SPC for RO desalination should be optimized based on the system recovery rate [5, 19].

An ERD is an essential component in modern RO plants for reducing the power consumption of seawater desalination and its effect should be included in the calculations of desalination energy [2, 20]. Three ERD efficiencies, 65% for turbo charger; 80% for Pelton wheel; 95% for pressure exchanger [2, 10, 21], were considered and the SPC was calculated for feed flow rates between 7 and 13 m$^3$/d (figure 3). For RO coupled with a 65% efficiency ERD system, the SPC increased gradually with the increase of recovery rate (figure 3 (a)). A similar trend was found for the RO membrane coupled with an ERD of 80 and 95% efficiency (figures 3 (b) and (c)). RO with ERD was more energy efficient than a RO system; for example, at 7 m$^3$/h feed flow rate, the SPC for the RO process without an ERD system reached an optimum value of 3.8 kWh/m$^3$ at 50% recovery rate (figure 2), whereas the corresponding values for RO with 65, 80, and 95% efficiency ERD were 2.58, 2.3, and 1.97 kWh/m$^3$, respectively (figure 3). Notably, almost 50% reduction in the desalination power consumption was achieved when the RO was coupled with ERD of 95% efficiency. Furthermore, the SPC was higher at higher feed flow rate because of the greater energy required for feed water pumping.

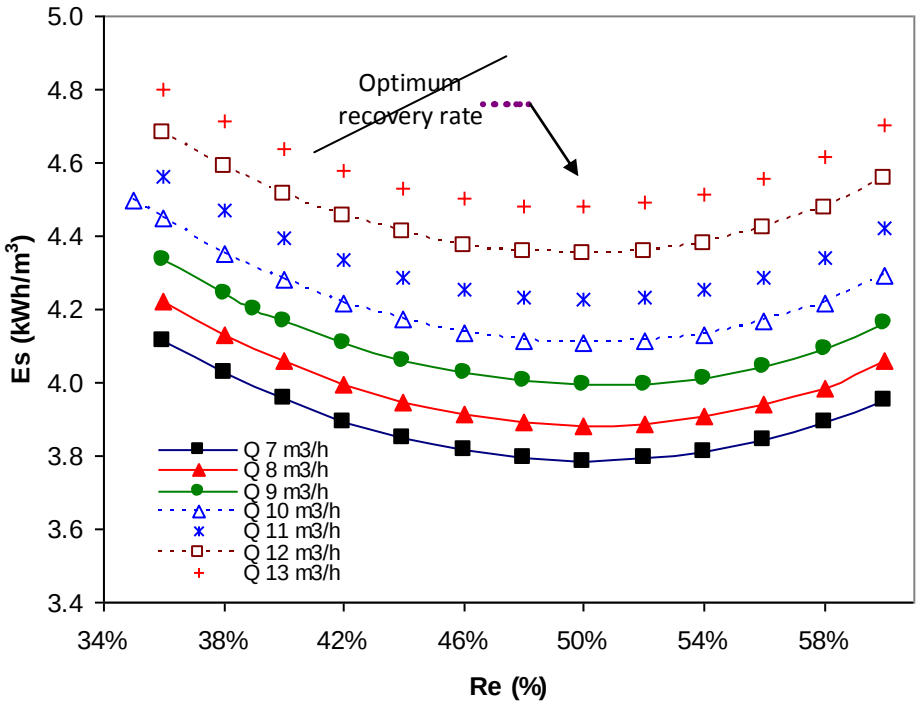


Figure 2: Impact of flow rate on the SPC of RO desalination at different recovery rates. The results are for SW30HRLE-440 RO module using a pressure vessel of 8 elements, feed temperature 25°C, and seawater salinity 35 g/L.

Although coupling RO with an ERD resulted in a decrease of the desalination energy, the SPC increased with the increase of recovery rate which disagreed with the findings of previous studies [5]. It is suggested that this was because ignoring the impact of an ERD system led to misinterpretation of the correlation between the SPC and RO recovery rate (which is illustrated in figure 2).

$E_{s\text{-}RO}$ was further analyzed by consideration of the SPC of high-pressure and booster pumps to better understand the impact of ERD efficiency on the performance of RO. According to equation (2), $E_{s\text{-}RO}$ can be also be expressed in terms of the SPC of the high-pressure and booster pumps as in equation 5:

$$E_{s-RO} = \left( \frac{P_{pp} * Q_p}{\eta * Q_p} + \frac{P_b * Q_c}{\eta * Q_p} \right) = \frac{P_{pp}}{\eta} + \frac{P_b * Q_c}{\eta * Q_p} = E_{pp} + E_{sb} \qquad [5]$$

The first term in equation (5), $E_{pp}$, represents the energy exerted by the high-pressure pump to raise seawater pressure to the feed pressure (line 1, Figure 1). The second term in equation (5), $E_{sb}$, is equal to the energy incurred by the booster pump to raise the pressure of seawater exiting the ERD to the feed pressure (line 5, figure 1).

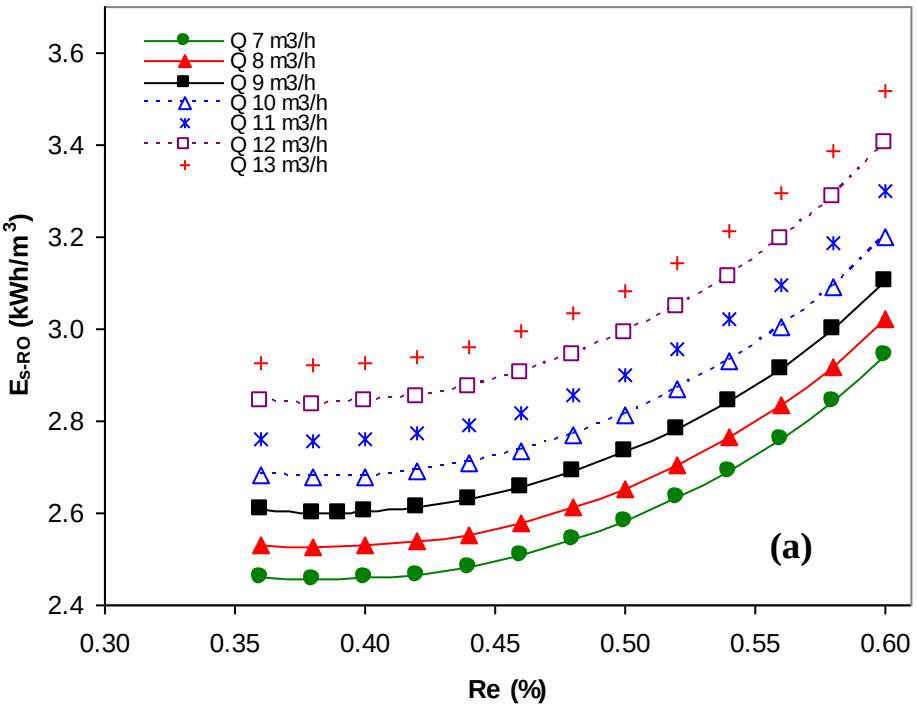


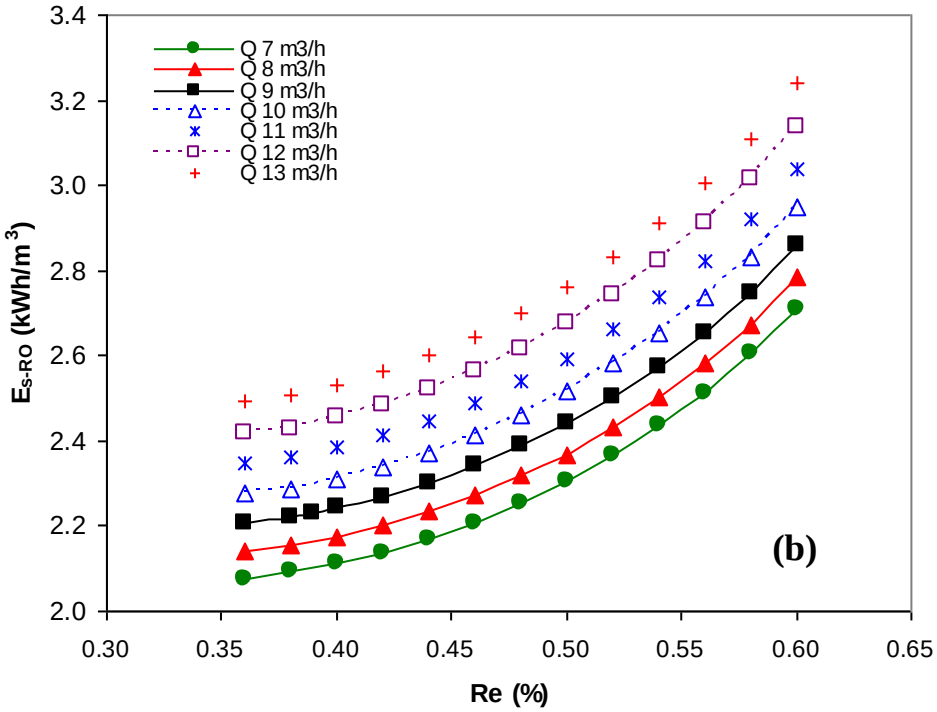

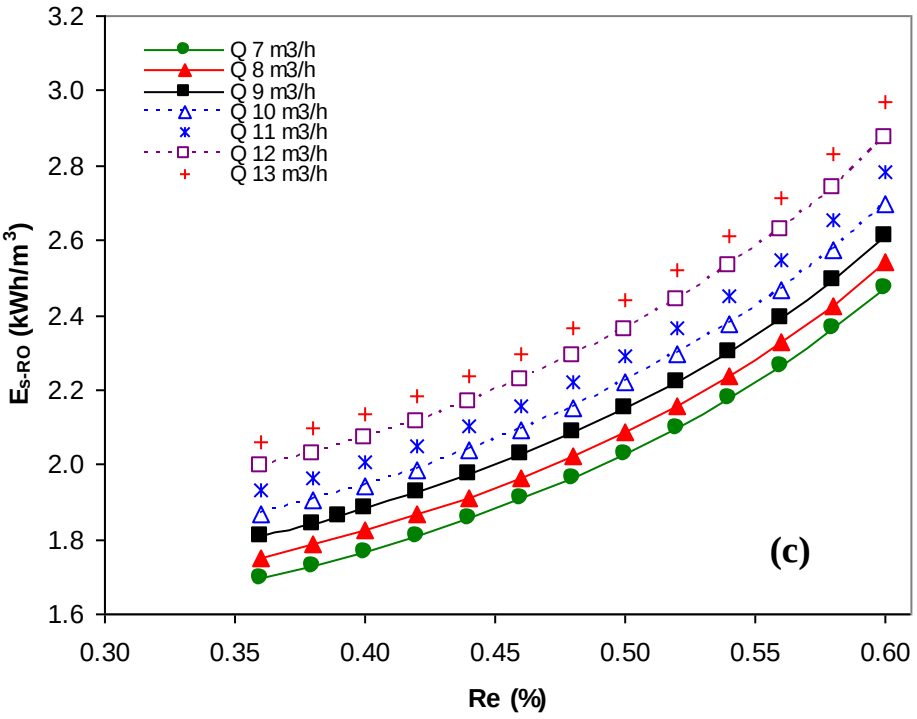


Figure 3: SPC of the RO membrane with an ERD system: (a) for RO with 65% ERD efficiency; (b) for RO with 80% ERD efficiency: (c) for RO with 95% ERD efficiency. Seawater salinity 35 g/L and feed temperature 25°C.

Figure 4 shows the SPC by the high-pressure pump, $E_{pp}$, for 7 $m^3$/h feed flow rate and 65, 80, and 95% ERD efficiencies. The results indicate that the impact of recovery rate on $E_{pp}$ was independent of the ERD efficiency and relied mainly on the feed pressure. $E_{pp}$ increased gradually with the increase of the RO recovery rate due to the high feed flow rate (figure 3) and the SPC by the high-pressure pump (line 1, figure 1). As the main contributor to the SPC of the desalination process, $E_{pp}$ was responsible for 60 to 96% of $E_{s\text{-}RO}$ in equation (5). At 36% recovery rate and 7 $m^3$/h feed flow rate, $E_{pp}$ was responsible for 60, 71, and 87% of $E_{s\text{-}RO}$ of RO coupled with 65, 80, and 95% ERD efficiency, respectively. The results suggested that $E_{pp}$ was responsible for most of $E_{s\text{-}RO}$ even at low recovery rates and this contribution increased with the recovery rate of RO process.

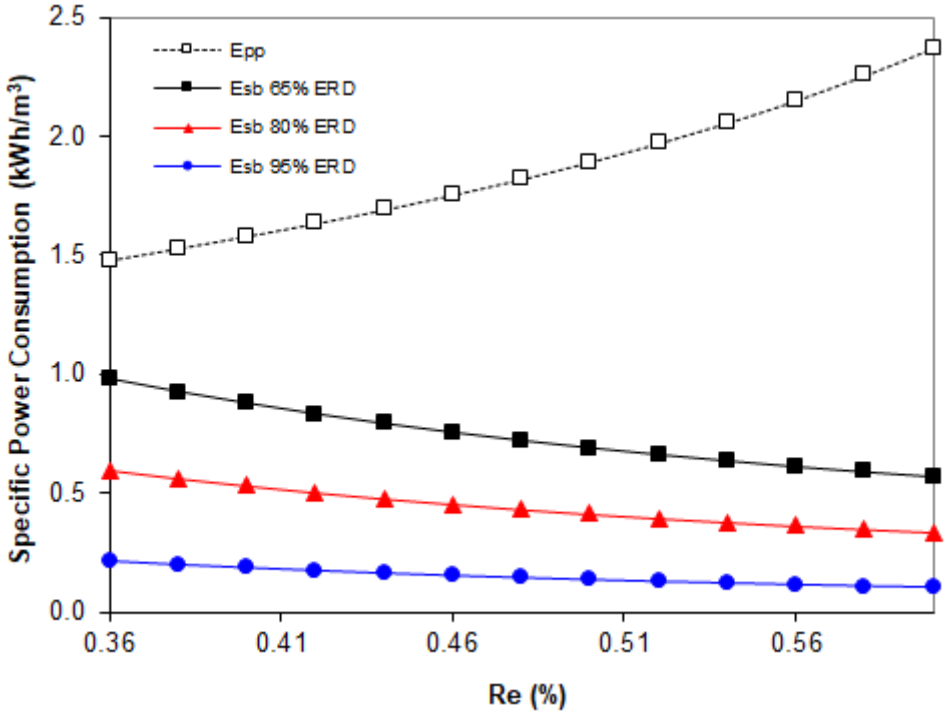


Figure 4: Energy requirements for seawater desalination by the high-pressure pump and booster pumps at 65, 80, and 95% ERD efficiencies; feed flow rate 7 $m^3$/h.

Interestingly, $E_{pp}$ contribution to $E_{s\text{-}RO}$ increased with the increase of ERD efficiency while $E_{sb}$ contribution to $E_{s\text{-}RO}$ decreased with the increase of ERD efficiency. $E_{sb}$ represented the energy exerted by the booster pump for seawater desalination, which was directly affected by the concentrate flow rate (line 7, figure 1). Opposite to $E_{pp}$, $E_{sb}$ decreased with the increase of RO recovery rate because of the lower concentrate flow rate to the booster pump. Technically, lower $E_{sb}$ can be achieved at high recovery rate and/or high ERD efficiency. In general, the contribution of $E_{sb}$ to $E_{s\text{-}RO}$ was less than 40% at 36% recovery rate and decreased to less than 20% at 60% recovery rate. The results also showed that the impact of $E_{sb}$ on $E_{s\text{-}RO}$ was more significant in the case of RO coupled with 65% ERD efficiency or when the RO was operating at low recovery rates. For example, increasing the recovery rate from 36 to 60% resulted in 0.1 kWh/$m^3$ increase of $E_{sb}$ for RO with 95% ERD efficiency, indicating that the insignificant impact of $E_{sb}$ on $E_{s\text{-}RO}$ when RO was coupled with a high-efficiency ERD. On the other hand, the impact of $E_{sb}$ became more significant at low recovery rate and/or ERD efficiency. From these results, it is recommended that RO be coupled with an ERD of high-efficiency (95%) when it is operated at low recovery rate. However, the SPC due to seawater pretreatment and brine discharge should be included to confirm these results.

### 3.2 Desalination Energy including Pretreatment and Brine Discharge

The energy requirements for seawater pretreatment and brine discharge were now included in calculations since they are essential parts of the RO process. According to equation (4b), $E_{st}$ is equal to the SPC of high-pressure pump ($E_{pp}$), booster pump ($E_{sb}$), pretreatment ($E_{spret}$), and brine discharge ($E_{sdis}$). At any feed flow rate, $E_{spret}$, $E_{sdis}$, and $E_{pp}$ are not affected by the efficiency of ERD, whereas $E_{sb}$ value varies with the ERD efficiency. $E_{st}$ was calculated for RO with an ERD of 65, 80, and 95% efficiencies and for feed flow rates between 7 and 13 $m^3$/h (figure 5). The results show that $E_{st}$ was higher at higher RO recovery rate and feed flow rates. Furthermore, the optimum value of $E_{st}$ was relatively dependent on the RO recovery rate, although it was highly affected by the efficiency of ERD system. This

optimum value occurred at a recovery rate of 48% for ERD of 65% efficiency and feed flow rates between 7 and 13 $m^3$/h. Taking an RO feed flow rate of 7 $m^3$/h as an example, for the RO coupled with a 65% efficiency ERD system, $E_{st}$ decreased at low and high recovery rates and reached an optimum value of 3.34 kWh/$m^3$ at 48% recovery rate (figure 5 (a)). In effect, $E_{st}$ increased between 6 and 7% over the optimum amount at 36 and 60% recovery rates, respectively. Operating the RO system at 50% recovery rate required $E_{st}$ of 3.35 kWh/$m^3$ which was only 0.02% more than the optimum $E_{st}$ value; that is, the increase of $E_{st}$ was insignificant. Although membrane fouling was out of the scope of this study, it should be noted that operating the RO at high recovery rates would increase the potential of membrane scaling especially on the last RO element in the pressure vessel which usually experiences high feed salinity [24-26].

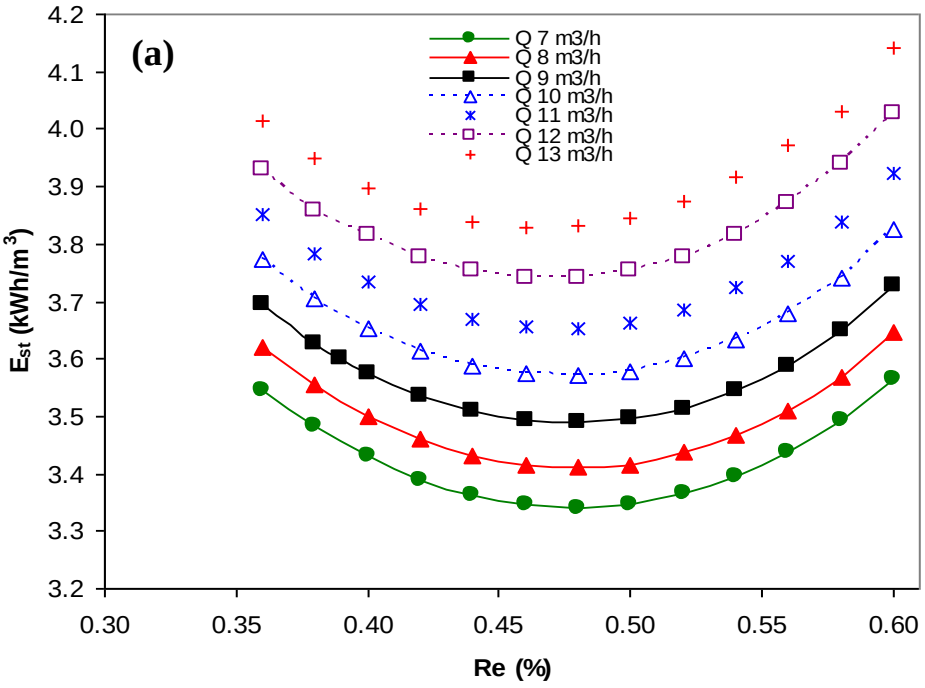

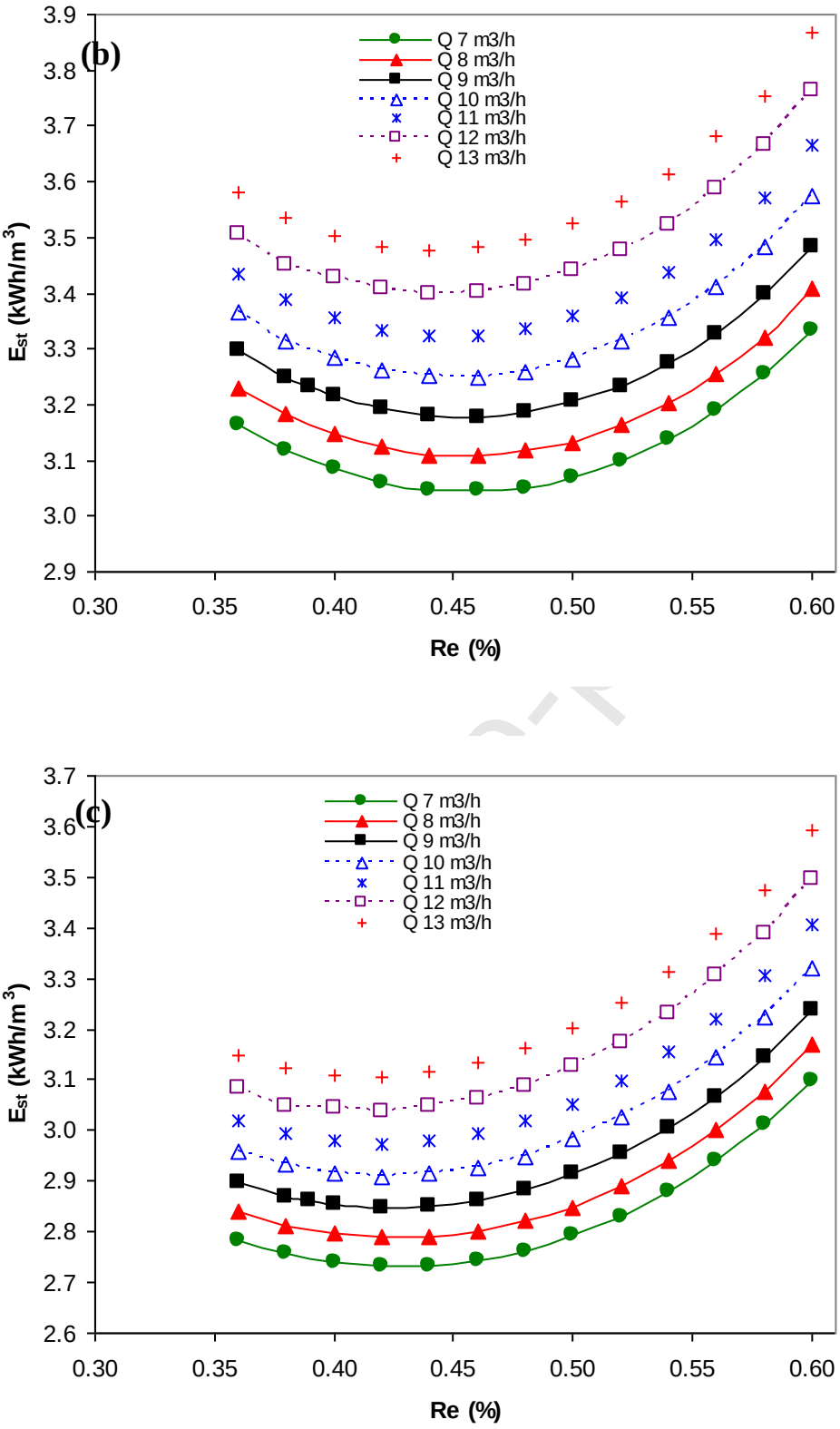


Figure 5: Impact of the RO recovery rate on the total desalination energy: (a) 65% ERD efficiency; (b) 80% ERD efficiency; (c) 95% ERD efficiency.

For the RO coupled with 80% efficiency ERD system, the RO recovery rate had lower impact on the optimum value of $E_{st}$ compared with the RO coupled with 65% efficiency ERD (figure

5 (b)). The optimum $E_{st}$ was even lower than that for the RO with 65% efficiency ERD and reached an optimum value at 46% recovery rate for all feed flow rates. For feed flow rate of 7 $m^3$/h and 46% recovery rate, $E_{st}$ was 3.05 kWh/$m^3$ but increased to 3.17 kWh/$m^3$ and 3.33 kWh/$m^3$ at 36% and 60% recovery rates, respectively. To operate the RO at 50% recovery rate, $E_{st}$ had to increase to 3.07 kWh/$m^3$ which was 0.8% higher than the optimum $E_{st}$ at 46% recovery rate. For the RO coupled with 95% ERD system, $E_{st}$ increased with the increase of recovery rate (figure 5 (c)). The optimum value of $E_{st}$ occurred at 42% recovery rate for all feed flow rates. The required $E_{st}$ for desalination at 7 $m^3$/h flow rate and 36% recovery rate was 2.78 kWh/$m^3$, which decreased to 2.73 kWh/$m^3$ at 42% recovery rate and reached 3.10 kWh/$m^3$ at 60% recovery rate. The results revealed that the optimum value of $E_{st}$ decreased as the efficiency of ERD increased from 65 to 95%. The optimum value of $E_{st}$ at feed flow rate of 7 $m^3$/h was 3.34 kWh/$m^3$ and 3.05 kWh/$m^3$ for 65 and 80% ERD efficiencies, respectively; the corresponding recovery rates were 48 and 46%, respectively. These latter recovery rates were lower than the target recovery rate of 50%. To achieve 50% recovery rate, the optimum $E_{st}$ should be increased by 2.2% which was higher than that for 65 and 80% ERD efficiencies. At 50% recovery rate, the required $E_{st}$ was 3.35, 3.07, and 2.79 kWh/$m^3$ for 65, 80, and 95% ERD efficiencies, respectively. Furthermore, the optimum recovery rates to achieve a minimum $E_{st}$ were 42, 46, and 48% for 95, 80, and 65% ERD efficiencies, respectively. In practice, recovery rates less than 50% were recommended in many RO pilot plants where high feed salinity and poor feed quality existed [34]. In such cases, ERD of 95% efficiency should be installed in order to operate at $E_{st}$ equal to/close to the minimum value which occurs at relatively low recovery rate (figure 5).

Figure 6 shows the ratio of $E_{pp}$, $E_{sb}$, $E_{spret}$, and $E_{sdis}$ to $E_{st}$ at 7 $m^3$/h feed flow rate and 50% recovery rate. $E_{pp}$ was responsible for the majority of SPC with 57 to 68% of $E_{st}$ followed by $E_{spret}$ between 21 and 25%, $E_{sb}$ between 5 and 21% of $E_{st}$, and $E_{sdis}$ with 2% of $E_{st}$. ERD impact on $E_{pp}$ increased with the efficiency increase from 65 to 95%, whereas this decreased with increasing efficiency of ERD for $E_{sb}$. This finding suggested that, at 95% ERD efficiency, $E_{sb}$ had insignificant impact on $E_{st}$.

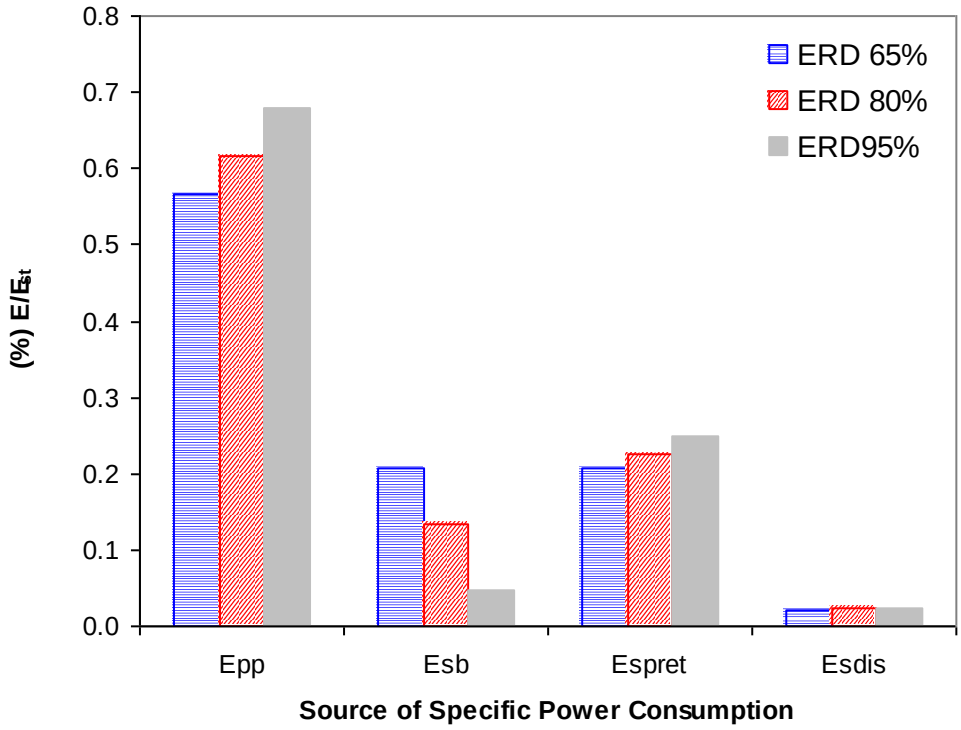


Figure 6: Specific power consumption by source, feed flow rate is 7 $m^3$/h and recovery rate 50%.

Interestingly, many RO desalination plants are designed to operate at fixed permeate flow rate, that is, capacity, which can be achieved at lower recovery rate by increasing the feed flow rate (figure 5). For example, RO should operate at 50 and 44% recovery rates at 7 and 8 $m^3$/h feed flow rates, respectively, to achieve permeate flow rate of 3. $m^3$/h. Practically, permeate flow rate can be controlled by adjusting a number of RO operating parameters such as feed pressure, feed flow rate, and recovery rate. For example, at a constant recovery rate, increasing the feed flow rate will result in a higher permeate flow; that is, $\mathrm{Re} = Q_p / Q_f$. As feed flow rate increases, the target permeate flow rate can be achieved by lowering the recovery rate. Thermodynamically, the minimum theoretical energy for desalination is proportional to the osmotic pressure of RO brine which has $C_c$ concentration as in equations 6 (a) and (b):

$$E_{mimi} \alpha C_c \qquad [6a]$$

$$E_{\min i} = \pi_c = \frac{\pi_f}{1 - \mathrm{Re}} \qquad [6b]$$

where, $E_{mini}$ is the minimum energy for RO desalination (kWh/$m^3$); $\pi_f$ is the osmotic pressure of feed solution (bar); and Re is the recovery rate of the RO unit (%). The term 1/1-Re in equation 4 represents the concentration factor, CF; hence, the concentration of RO brine can be calculated as shown in equations 7 (a) and (b):

$$C_c = \frac{C_f}{1 - \mathrm{Re}} \qquad [7a]$$

$$C_c = C_f * CF \quad [7b]$$

where $C_f$ is the concentration of feed solution (mol/L). The osmotic pressure of RO brine, $\pi_c$, can be estimated from Van't Hoff equation, using equation (7b) to represent the concentration of the RO brine as shown in equation 8:

$$\pi_c = n * R * C_f * CF * T \quad [8]$$

where n is the number of ions in solution; $R$ is the universal gas constant (~0.083L·atm/K·mol); and $T$ is the temperature in Kelvin (273 + $^{o}$C). In equation (6b), $E_{mini}$ can be expressed as illustrated in equation 9:

$$E_{\min i} = n * R * C_f * CF * T \quad [9]$$

Equation 9 shows that $E_{mini}$ is a function of the concentration factor, CF; any variation of the CF would therefore result in a direct change of the $E_{mini}$ value. Figure 7 shows the impact of feed flow rate on the concentration factor at a constant permeate flow rate, $Q_p$.

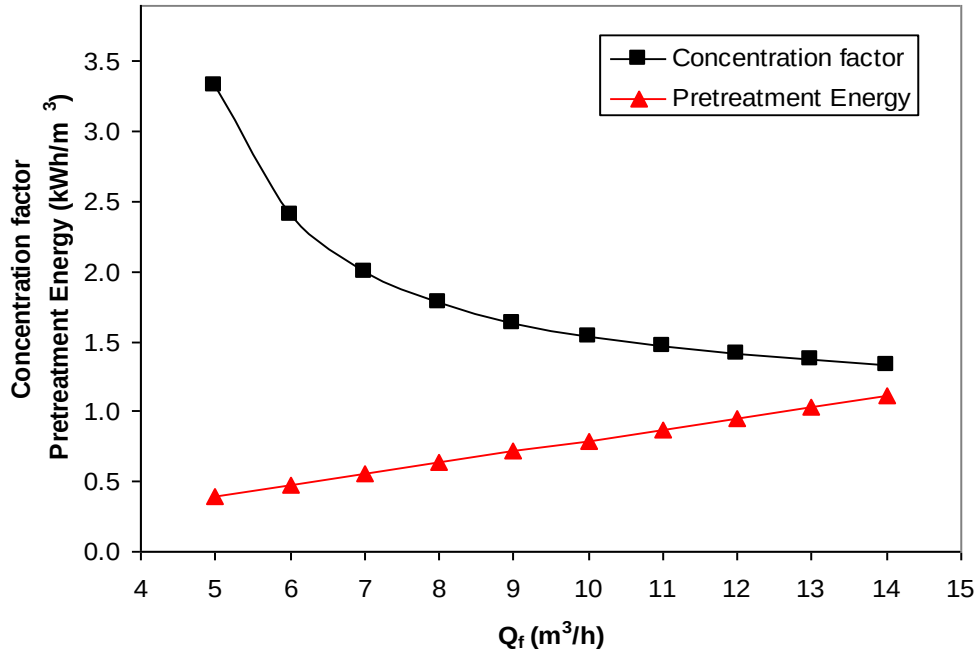


Figure 7: Impact of feed flow rate on the minimum desalination energy and concentration; results were obtained at 35 g/L seawater salinity, 25$^{o}$C feed temperature, and 3.5 m$^3$/h permeate flow rate. Pretreatment energy was based on intake, pretreatment processes, and supply.

The concentration factor, CF, decreased from 3.3 to 1.3 with the increase of feed flow rate from 5 to 13 m$^3$/h. The recovery rate of RO system was inversely related to the feed flow rate as shown in equations 10 (a), (b) and (c);

$$\mathrm{Re} \alpha \frac{1}{Q_f} \quad [10a]$$

$$C_c = \frac{C_f}{1-\mathrm{Re}} \quad [10b]$$

$$C_c = \frac{C_f}{1-\frac{Q_p}{Q_f}} \quad [10c]$$

RO recovery rate can be decreased with an increase of the feed flow rate to maintain a constant permeate flow rate. Re decrease would result in a simultaneous decrease of the concentration of RO brine [equation (10b)] as well as the minimum desalination energy [equation (6b)], suggesting that $E_{min}$ decreases at higher feed flow rate [equation (10c)]. Although this was theoretically viable, practically, high feed flow rate would increase the pretreatment energy which negatively affected the desalination energy. As shown in figure 7, the pretreatment power consumption increased with the increase of the feed flow rate, $Q_f$. Pretreatment power consumption impacts the overall desalination energy and, hence, should be taken into account upon considering high feed flow rates.

Figure 8 shows the total desalination energy, $E_{st}$, at different feed flow rates and fixed permeate flow rate, $Q_p$, of 3.5 $m^3$/h. Feed flow rate increased from 7 to 12 $m^3$/h, whereas the recovery rate decreased to maintain a constant $Q_p$ of 3.5 $m^3$/h. In general, $E_{st}$ increased with the increase of feed flow rate at all ERD efficiencies but was higher for the RO coupled with 65% efficiency ERD system because of the lower energy recovery compared to the RO coupled with 80 and 95% efficiency ERD system. One of the interesting findings in figure 8 was that the required recovery rate of RO to maintain a constant permeate flow rate of 3.5 $m^3$/h decreased with the increase of the feed flow rate. Operating at lower recovery rate decreased the required feed pressure for seawater desalination because of the lower CF according to equation (10b). For example, to produce 3.5 $m^3$/h of product water at 7 $m^3$/h feed flow rate, the recovery rate of the RO should be 50%, whereas a recovery rate of 44% would be enough to reach the same permeate flow rate at 8 $m^3$/h feed flow rate (figure 8). The corresponding $E_{st}$ values for 65% ERD efficiency were 3.35 and 3.43 kWh/$m^3$, respectively. $E_{st}$, however, decreased to 2.79 kWh/$m^3$ for ERD with 95% efficiency at 7 and 8 $m^3$/h flow rates but slightly increased 2.86 kWh/$m^3$ at 9 $m^3$/h flow rate (figure 8).

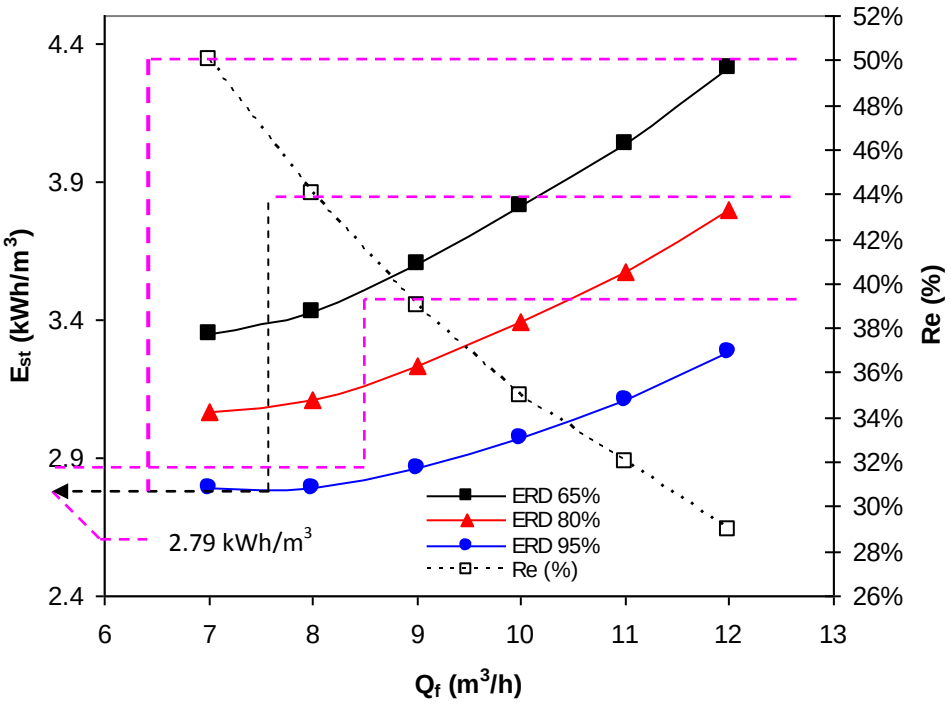


Figure 8: Total desalination energy at different feed flow rates and ERD efficiencies, permeate flow rate at all recovery rates is 3.5 $m^3$/h.

This result suggested that operating RO at high feed flow rate was a feasible option particularly when it was coupled with 95% ERD efficiency. Slightly higher $E_{st}$ was incurred, about 0.07 kWh/$m^3$, when the feed flow rate increased from 7 to 9 $m^3$/h, but this will be mitigated over the membrane life time due to lower fouling propensity. Previous studies showed that membrane fouling results in an annual flux decline up to 10% which increases the desalination energy [20, 28]. At a fixed permeate flow rate, feed flow rate can be optimized to meet the designed permeate flow rate. According to equation (10b), this strategy will reduce the brine concentration and hence the feed pressure, which is responsible for membrane compaction [29-32]. Secondly, lower brine concentration can reduce scale formation due to the deposition of sparingly soluble metal ions on the membrane surface [25-27]. As shown in figure 7, concentration factor (CF) decreased with the increase of feed flow rate ($Q_f$) which is an indicator of lower brine concentration [equation (7b)]. This parameter is particularly important for the tail RO elements in the pressure vessel which undergoes scale fouling more than other elements due to the high feed concentration present. Finally, using high feed flow rate will reduce the concentration of RO brine for discharge and the impact of desalination process on the environment upon discharge to the sea.

### 3.3 Distribution of SPC in Pressure Vessel

Although it is desirable to have an even recovery rate across the RO modules in the pressure vessel, it is difficult to achieve that situation practically. In the pressure vessel, feed concentration increases from the first to last RO module, whereas recovery rate decreases due to larger osmotic pressure of the feed concentration [33-34]. Feed pressure also slightly decreases along the pressure vessel from the first to the last element due to the pressure drop. Uneven distribution of feed pressure and concentration affects the energy incurred by each RO module particularly the last RO module which is prone to scale fouling. The design criteria of RO system are to deliver a certain amount of desalinated water; hence, the

recovery rate of the RO can be decreased at high feed flow rate without compromising the permeate flow rate. We calculated the net SPC per RO module, $E_{sN}$, for each RO element in the pressure vessel at 7, 8, and 9 $m^3$/h to understand $E_{sN}$ distribution across the pressure vessel. $E_{sN}$ represents the specific power consumption per RO module and it is calculated from equation 11:

$$E_{sN} = \frac{E_{sG} * E_s}{E_{sGt}} \quad [11]$$

where $E_{sG}$ is the gross specific power consumption per RO module; $E_s$ is the specific power consumption of the RO system [equation (1)]; and $E_{sGt}$ is the total gross specific power consumption of the RO system. $E_{sG}$ and $E_{sGt}$ were calculated from equations 12 & 13:

$$E_{sG} = \frac{P_{fi} * Q_{fi}}{Q_{pi}} \quad [12]$$

$$E_{sGt} = \sum_{i=1}^{i=n} \frac{P_{fi} * Q_{fi}}{Q_{pi}} \quad [13]$$

where $P_{fi}$ is the feed pressure at element $i$ in the pressure vessel (bar); $Q_{fi}$ is the feed flow rate of element $i$ in the pressure vessel ($m^3$/h); $n$ is the number of the RO modules in the pressure vessel; $Q_{pi}$ is the permeate flow rate of element $i$ in the pressure vessel ($m^3$/h). Substituting equations (12) and (13) into equation (11) to calculate $E_{sN}$ gives equation 14:

$$E_{sN} = \frac{\frac{P_{fi} * Q_{fi}}{Q_{pi}} * E_s}{\sum_{i=1}^{i=n} \frac{P_{fi} * Q_{fi}}{Q_{pi}}} \quad [14]$$

ROSA software was used to calculate $P_{fi}$, $Q_{fi}$ and $Q_{pi}$ of RO module $i$ in the pressure vessel. Tables 1–3 show $P_{fi}$, $Q_{fi}$, and $Q_{pi}$ of the RO system at 7, 8. and 9 $m^3$/h, respectively. The recovery rate of each RO module, $Re_{mod}$, in the pressure vessel was calculated as the ratio of $Q_{pi}$ to $Q_f$ as in equation 15:

$$\mathrm{Re}_{\mathrm{mod}} = \frac{Q_{pi}}{Q_f} \quad [15]$$

At 7 $m^3$/h feed flow rate, $Re_{mod}$ were 14 and 1% for the lead and tail RO modules in the pressure vessel, respectively; this result shows the significant variation in the RO recovery rate between the lead and tail elements. The high feed concentration of the last RO module resulted in a small percentage recovery rate of 1% due to the high feed concentration (figure 9 (a)). The feed concentration, $C_f$, increased from lead to tail RO elements in the pressure vessel but was higher at lower RO feed flow rates. Practically, the higher the feed concentration is, the higher the membrane scale fouling will be due to the precipitation of sparingly soluble salts [35-36]. As the feed flow rate increased to 8 $m^3$/h, $Re_{mod}$ of the lead and tail RO modules were 11 and 2%, respectively. Compared to 7 $m^3$/h feed flow rate, operating at 8 $m^3$/h feed flow rate doubled the recovery rate of the tail element while

increasing the feed flow rate of the tail elements by 28%. The increase of feed flow rate has the potential of reducing the scale fouling due to the lower brine concentration [equation (10c)].

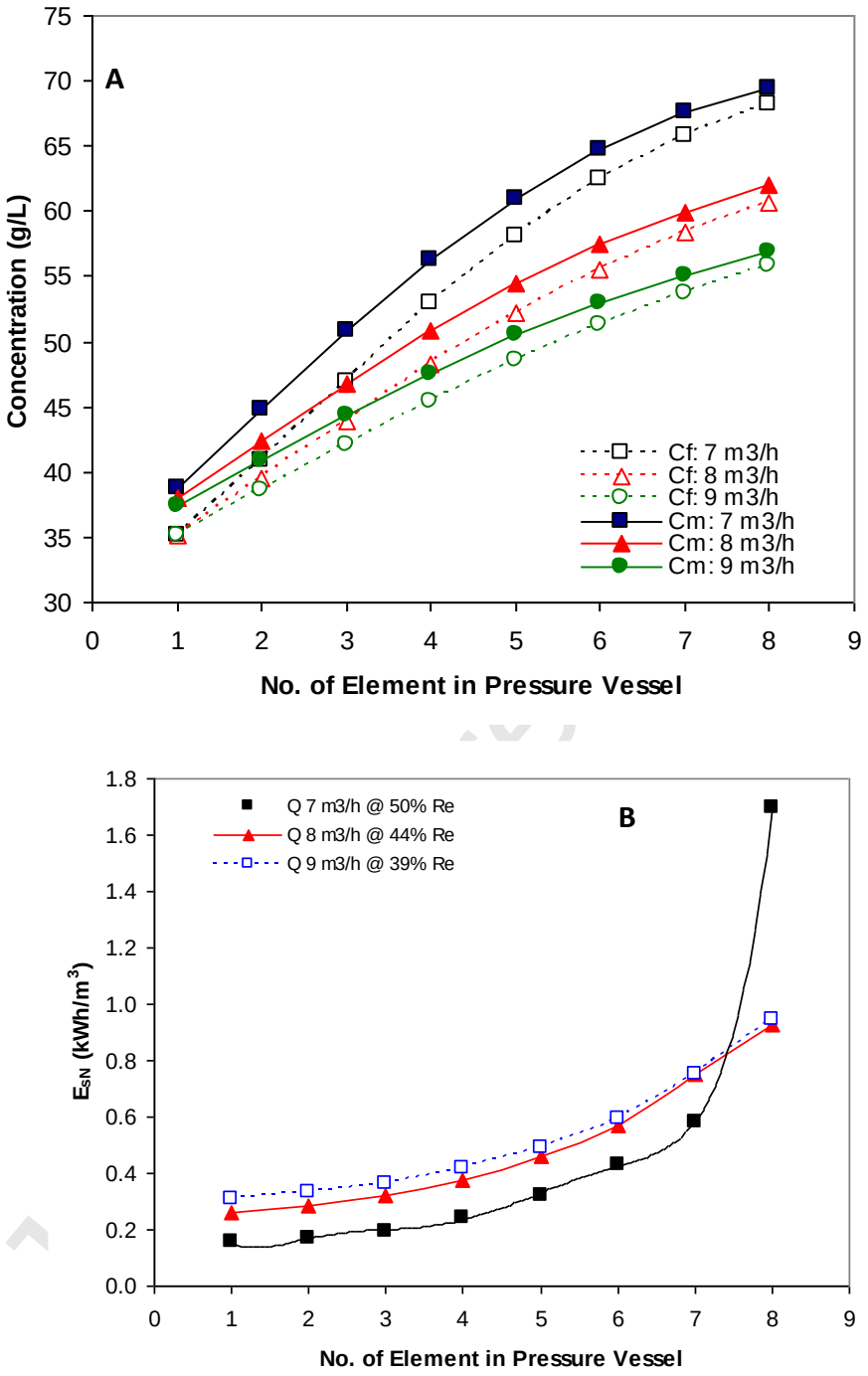


Figure 9: Feed concentration and total desalination energy across the RO pressure vessel: (A) concentration of RO brine; (B) total desalination energy of each RO module. Initial feed seawater concentration is 35 g/L.

The results also show that RO recovery rate was more evenly distributed across the RO elements in the pressure vessel for the 8 $m^3$/h feed flow rate. Similarly, for the 9 $m^3$/h feed flow rate, more even distribution of the recovery rate was observed throughout the RO modules [Tables 1 to 3]. Increasing the feed flow rate reduced the feed concentration to the RO modules and resulted in more even distribution of the recovery rate. The drawback of

increasing the feed flow rate was reflected on $E_{st}$. However, for 95% efficiency ERD, $E_{st}$ remained unchanged when the feed flow rated increased to 8 $m^3$/h; this result emphasized the importance of using high-efficiency ERD. As the feed flow rate increased to 9 $m^3$/h, $E_{st}$ slightly increased to 2.86 kWh/$m^3$. Compared to the 8 $m^3$/h feed flow rate, $Re_{mod}$ of the last two elements remained 2% when the feed flow rate increased to 9 $m^3$/h but it was more evenly distributed across the lead RO elements [Tables 1 to 3]. The concentration at the membrane surface, $C_m$ (g/L), was calculated and presented in figure 9 (a). $C_m$ represents the actual feed concentration at the membrane surface which was calculated from equations 16 (a) and (b):

$$CP = \frac{C_m - C_p}{C_B - C_p} \quad [16a]$$

$$C_m = [(C_B - C_p) * CP] + C_p \quad [16b]$$

where $C_B$ is the bulk concentration of feed solution (g/L); $C_p$ is the permeate concentration (g/L); and $CP$ is the concentration polarization factor. CP for 8-inch RO element was calculated following the empirical formula provided in equation 17 [16]:

$$CP = e^{(0.7\,\mathrm{Re})} \quad [17]$$

Feed concentration at the membrane surface is always higher than that at the bulk solution because of the concentration polarization phenomenon [15, 17. 33]. CP increases with the recovery rate of the RO membrane, that is, higher at the lead element than at the tail element. The difference between the feed concentration, $C_f$, and concentration at the membrane surface, $C_m$, was between 10 and 6.5% for feed flow rates between 7 and 9 $m^3$/h; the lowest CP of 6.5% was for the 9 $m^3$/h flow rate (figure 9 (a)). Increasing the feed flow rate resulted in more even distribution of feed flow across the pressure vessel and increased the recovery rate of the tail element. This caused a slight CP increase of the tail element (2%) for the 9 $m^3$/h flow rate compared to the 7 $m^3$/h flow rate (1.75%). However, $C_m$ at the tail element decreased by 18%, from 69.5 to 56.9 g/L, by increasing the feed flow rate from 7 to 9 $m^3$/h. On the other hand, $C_m$ at the tail element decreased by 11%, from 69.5 to 62 g/L, when the feed flow rate increased from 7 to 8 $m^3$/h while the increase of CP at tail RO element was insignificant. Reducing the feed concentration of the tail element has the potential of minimizing the incidence of scale fouling [25-27]. In the long term, this will ensure an energy efficient and smooth RO operation. Previous studies showed that membrane fouling results in a flux decline over time [20] and simultaneous increase of the power consumption of the RO process. This is another advantage of increasing the flow rate of RO feed solution, but the benefit will be more obvious when a high-efficiency ERD system is applied for energy recovery. Compared to 7 $m^3$/h flow rate, using 8 $m^3$/h flow rate and ERD of 95%, efficiency has the potential of reducing the $C_m$ of the tail element, whereas $E_{st}$ remains unaffected (2.79 kWh/$m^3$).

$E_{sN}$ is the net specific power consumption per RO element in the pressure vessel. Regardless of the feed flow rate, $E_{sN}$ increased gradually from element 1 to 8 because of the high feed concentration and low recovery rate of the tail elements [Tables 1 to 3]. At 7 $m^3$/h and 50% recovery rate, $E_{sN}$ of 0.16 kWh/$m^3$ was incurred at the first RO element and increased to 1.69 Wh/$m^3$ at the tail RO elements in the pressure vessel (figure 9 (b)); that is, $E_{sN}$ of the lead RO element was 10 times lower than that of the tail RO element. At 8 $m^3$/h and 44% recovery

rate, $E_{sN}$ increased to lesser extent from the first to the tail RO element in the pressure vessel; $E_{sN}$ of the lead element was 3.5 times higher than that of the tail RO element indicating more even energy distribution throughout the RO elements in the pressure vessel. Similarly, for 9 $m^3$/h and 39% recovery rate, $E_{sN}$ of the lead element was 3 times higher than that at the tail RO element due to the better distribution of the permeate flow across the RO elements.

Table 1: Performance of RO modules in the pressure vessel; Es values were 3.79 kWh/$m^3$, 3.95 kWh/$m^3$, and 4.20 kWh/$m^3$ for RO system with feed flow rate 7 $m^3$/h.

| Elem. No | $Q_{pi}$ ($m^3$/h) | $Q_{fi}$ ($m^3$/h) | $P_{fi}$ (bar) | $Re_{mod}$ (%) | $E_{sG}$ (kWh/$m^3$) | $E_{sN}$ (kWh/$m^3$) |
|---|---|---|---|---|---|---|
| 1 | 0.99 | 7.00 | 54.18 | 0.14 | 13.30 | 0.16 |
| 2 | 0.78 | 6.01 | 54.00 | 0.11 | 14.45 | 0.17 |
| 3 | 0.59 | 5.24 | 53.85 | 0.08 | 16.61 | 0.20 |
| 4 | 0.42 | 4.65 | 53.73 | 0.06 | 20.66 | 0.24 |
| 5 | 0.29 | 4.23 | 53.63 | 0.04 | 27.16 | 0.32 |
| 6 | 0.2 | 3.93 | 53.54 | 0.03 | 36.53 | 0.43 |
| 7 | 0.14 | 3.73 | 53.45 | 0.02 | 49.45 | 0.58 |
| 8 | 0.09 | 3.59 | 53.37 | 0.01 | 144.13 | 1.69 |

Table 2: Performance of RO modules in the pressure vessel; Es values were 3.79 kWh/$m^3$, 3.95 kWh/$m^3$, and 4.20 kWh/$m^3$ for RO system with feed flow rate 8 $m^3$/h.

| Elem. No | $Q_{pi}$ ($m^3$/h) | $Q_{fi}$ ($m^3$/h) | $P_{fi}$ (bar) | $Re_{mod}$ (%) | $E_{sG}$ (kWh/$m^3$) | $E_{sN}$ (kWh/$m^3$) |
|---|---|---|---|---|---|---|
| 1 | 0.880 | 8.00 | 49.66 | 0.11 | 15.68 | 0.26 |
| 2 | 0.720 | 7.12 | 49.45 | 0.09 | 16.98 | 0.28 |
| 3 | 0.570 | 6.40 | 49.26 | 0.07 | 19.20 | 0.32 |
| 4 | 0.440 | 5.82 | 49.10 | 0.06 | 22.55 | 0.38 |
| 5 | 0.330 | 5.38 | 48.95 | 0.04 | 27.71 | 0.46 |
| 6 | 0.250 | 5.05 | 48.82 | 0.03 | 34.24 | 0.57 |
| 7 | 0.180 | 4.80 | 48.70 | 0.02 | 45.09 | 0.75 |
| 8 | 0.140 | 4.62 | 48.59 | 0.02 | 55.68 | 0.93 |

Table 3: Performance of RO modules in the pressure vessel; Es values were 3.79 kWh/$m^3$, 3.95 kWh/$m^3$, and 4.20 kWh/$m^3$ for RO system with feed flow rate 9 $m^3$/h.

| Elem. No | $Q_{pi}$ ($m^3$/h) | $Q_{fi}$ ($m^3$/h) | $P_{fi}$ (bar) | $Re_{mod}$ (%) | $E_{sG}$ (kWh/$m^3$) | $E_{sN}$ (kWh/$m^3$) |
|---|---|---|---|---|---|---|
| 1 | 0.81 | 9.00 | 46.85 | 0.09 | 18.07 | 0.31 |
| 2 | 0.68 | 8.19 | 46.59 | 0.08 | 19.48 | 0.33 |
| 3 | 0.56 | 7.51 | 46.36 | 0.06 | 21.59 | 0.37 |
| 4 | 0.45 | 6.95 | 46.16 | 0.05 | 24.75 | 0.42 |
| 5 | 0.36 | 6.50 | 45.97 | 0.04 | 28.82 | 0.49 |
| 6 | 0.28 | 6.15 | 45.80 | 0.03 | 34.93 | 0.59 |
| 7 | 0.21 | 5.87 | 45.64 | 0.02 | 44.30 | 0.75 |
| 8 | 0.16 | 5.65 | 45.49 | 0.02 | 55.78 | 0.95 |

In practical terms, increasing the feed flow rate can be performed to enhance the performance of the RO-ERD system; in the long term, this strategy provides more smooth and stable RO operating conditions and reduces the potential of scale fouling. The net SPC and recovery rate per RO module was more evenly distributed across the RO elements in the pressure vessel at higher RO feed flow rates. This was particularly applicable for RO coupled with a high-efficiency ERD. The total power consumption for desalination, including pretreatment and brine discharge, could be kept constant or slightly decreased as feed flow rate increases for the RO coupled with ERD of 80% efficiency or higher.

## 4. Conclusions

The energy requirements for RO seawater desalination continue to be a major issue of debate. This study analyzed the power consumption of the RO process including the ERD system and also the pretreatment process. The results showed that the optimum power consumption for seawater desalination was dependent on the RO recovery rate when the RO membrane was coupled with an ERD system. However, the optimum power consumption for desalination became relatively reliant on the RO recovery rate when the pretreatment energy was added. The total desalination energy, including pretreatment, reached an optimum value at 48, 46, and 42% recovery rates for RO coupled with an ERD of 65, 80, and 95% efficiency, respectively. These results suggested that the RO-ERD system can be designed to operate at different optimum recovery rates. As such, one of the main conclusions of this investigation was that the feed flow rate can be increased to meet the optimum recovery rate and projected permeate flow rate of the RO system. Operating at high feed flow rate showed the potential of reducing the total energy requirements for desalination when the RO was coupled with ERD of 95% efficiency. On the other hand, these outlined conditions have the advantage of reducing RO scale fouling due to the precipitation of sparingly soluble salts. It was shown that increasing the RO feed flow rate helped to distribute the RO system recovery rate more evenly across the pressure vessel. Therefore, it was recommended to use high-efficiency ERD such as pressure exchanger in conjunction with the RO desalination system, which allows increasing the feed flow rates without compromising the desalination energy requirements.

## Conflict of Interest

The authors of the present work declare no conflict of interest.

## 5. Acknowledgements

The authors would like to acknowledge School of Civil and Environmental Engineering at the University of Technology in Sydney, University of Surrey in United Kingdom and the Public Authority for Applied Education and Training (PAAET) at Kuwait for their assistance in completing this study during the Sabbatical leave.

## 6. References

[1] Adnan Ahmad, Fahad Jamshed, Tabinda Riaz, Sabad-e- Gul, Sidra Waheed, Aneela Sabir, Adnan Alhathal Alanezi, Muhammad Adrees, Tahir Jamil, Self-sterilized composite membranes of cellulose acetate/polyethylene glycol for water desalination, Carbohydrate Polymers, 149 (2016) 207-216.

[2] Gude V.G., Energy consumption and recovery in reverse osmosis, Desalination and Water Treatment, 36 (2011) 239-260.

[3] Mingheng Li, Predictive modeling of a commercial spiral wound seawater reverse osmosis module, Chemical Engineering Research and Design, Volume 148, 2019, Pages 440-450, ISSN 0263-8762, https://doi.org/10.1016/j.cherd.2019.06.033.

[4] Peñate B., García-Rodríguez L., Energy optimisation of existing SWRO (seawater reverse osmosis) plants with ERT (energy recovery turbines): Technical and thermoeconomic assessment, Energy, 36 (2011) 613-626.
[5] Mark Wilf, Kenneth Klinko, Optimization of seawater RO systems design, Desalination, V 138 (2001), 299-306.
[6] David M. Warsinger, Emily W. Tow, Kishor G. Nayar, Laith A. Maswadeh, John H. Lienhard V, Energy efficiency of batch and semi-batch (CCRO) reverse osmosis desalination, Water Research, V 106 (2016), 272-282
[7] Vanessa Haluch, Everton F. Zanoelo, Christian J.L. Hermes, Experimental evaluation and semi-empirical modeling of a small-capacity reverse osmosis desalination unit, Chemical Engineering Research and Design, Volume 122, 2017, Pages 243-253, ISSN 0263-8762, https://doi.org/10.1016/j.cherd.2017.04.006.
[8] Meng Shen, Sinan Keten, Richard M. Lueptow, Rejection mechanisms for contaminants in polyamide reverse osmosis membranes, Journal of Membrane Science, V 509 (2016), 36-47.
[9] Baltasar Peñate, Lourdes García-Rodríguez, Current trends and future prospects in the design of seawater reverse osmosis desalination technology, Desalination, V 284, 2012, 1–8.
[10] Filmtec Reverse Osmosis Membranes, Technical Manual, http://msdssearch.dow.com/PublishedLiteratureDOWCOM/dh_095b/0901b8038095b91d.pdf?filepath=/609-00071.pdf&fromPage=GetDoc , accessed on 29/08/2017.
[11] Stover R.L., Seawater reverse osmosis with isobaric energy recovery devices, Desalination, 203 (2007) 168-175.
[12] Ali Altaee, Adnan Alhathal Alanezi, Radhi Alazmi, Alaa H. Hawari, and Claudio Mascialino Chapter 6: Effect of the Draw Solution on the Efficiency of Two-Stage FO-RO/BWRO for Seawater and Brackish Water Desalination, *Section (ii) Freshwater by Desalination*, Water Management Social and Technical Perspectives, Green Chemistry and Chemical Engineering, CRC Press, Tailor & Francis Group 2018.
[13] Mamo J., Pikalov V., Arrieta S., Jones A.T., Independent testing of commercially available, high-permeability SWRO membranes for reduced total water cost, Desalination and Water Treatment, 51 (2013) 184-191.
[14] James K. Edzwald, Johannes Haarhoff, Seawater pretreatment for reverse osmosis: Chemistry, contaminants, and coagulation, Water Research, V 45 (2011), 5428-5440
[15] A.J. Karabelas, C.P. Koutsou, M. Kostoglou, D.C. Sioutopoulos, Analysis of specific energy consumption in reverse osmosis desalination processes, Desalination, accepted 3/05/2017
[16] Ali Altaee, Theoretical study on feed water designs to reverse osmosis pressure vessel, Desalination, V 326 (2013), 1-9.
[17] Ali Altaee, Computational Model for Estimating Reverse Osmosis System Design and performance: Part-One Binary Feed Solution, Desalination, V 291 (2012), 101-105.
[18] Rami Salah El-Emam, Ibrahim Dincer, Thermodynamic and thermoeconomic analyses of seawater reverse osmosis desalination plant with energy recovery, Energy, V 64 (2014), 154–163
[19] Ali Altaee, Forward Osmosis: Potential use in Desalination and Water Reuse, Journal of membrane and Separation Technology, 1 (2012), 79-93
[20] Ali Altaee, Graeme Millar, Guillermo Zaragoza, Adel Sharif, Energy Efficiency of RO and FO-RO system for High Salinity Seawater Treatment, Clean Technology and Environmental Policy, doi: 10.1007/s10098-016-1190-3
[21] Tianyu Qiu and Philip A. Davies, Comparison of Configurations for High-Recovery Inland Desalination Systems, Water, V (4), 690-706

[22] Seungwon Ihm, Othman Y. Al-Najdi, Osman A. Hamed, Gabjin Jun, Hyunchul Chung, Energy cost comparison between MSF, MED and SWRO: Case studies for dual purpose plants, Desalination, V 397 (2016), 116–125
[23] P. Corsin, G. Cartier and C. Masson, Pumps in seawater reverse osmosis, http://www1.cetim.fr/eemods09/pages/programme/051-Corsin-final.pdf , accessed on 2/1/2017.
[24] Silvia Gallego, Fernando del Vigo, Steve Chesters, PRACTICAL EXPERIENCE WITH HIGH SILICA CONCENTRATION IN RO WATERS, WIM 2008 International Congress on water management in the mining industry. Santiago Chile July 9-11th 2008 REF: WIM08-53
[25] Stephen P.Chesters, Matthew W. Armstrong, RO Membrane Cleaning–explaining the science behind the art, The International Desalination Association World Congress on Desalination and Water Reuse 2013 / Tianjin, China REF: IDAWC/TIAN13-435
[26] Zhixin Hu, AliceAntony, GregLeslie, PierreLe-Clech, Real-time monitoring of scale formation in reverse osmosis using electrical impedance spectroscopy, Journal of Membrane Science, V 453 (2014), 320–327
[27] Ruth Kaplan, Darryl Mamrosh, Hafiz H. Salih, Seyed A. Dastgheib, Assessment of desalination technologies for treatment of a highly saline brine from a potential $CO_2$ storage site, Desalination V 404 (2017), 87–101
[28] Hydranautics Design Limits, Hydranautics Nito Dinko, www.membranes.com/docs/trc/Dsgn_Lmt.pdf , accessed on 15/12/2016
[29] Alice Antony, AmosBranch, GregLeslie, PierreLe-Clech, Impact of membrane ageing on reverse osmosis performance–Implications on validation protocol, Journal of Membrane Science, V 520 (2016), 37–44
[30] Ronan Killian McGovern, Dillon McConnon and John H. Lienhard V, The Effect of Very High Hydraulic Pressure on the Permeability and Salt Rejection of Reverse Osmosis Membranes, The International Desalination Association World Congress on Desalination and Water Reuse 2015/San Diego, CA, USA REF: IDAWC15
[31] H. Kotb, E.H. Amer, K.A. Ibrahim, On the optimization of RO (Reverse Osmosis) system arrangements and their operating conditions, Energy, V 103 (2016), 127–150
[32] S.M.Javaid. Zaidi, F. Fadhillah, Z. Khan, A. F. Ismail, Salt andwater transport in reverse osmosis thin film composite seawater desalination membranes, Desalination, V 368 (2015), 202–213
[33] Ali Altaee, A Computational Model to Estimate the Performance of 8 inches RO Membranes in Pressure Vessel, Journal of Membrane and Separation Technology, 19 (2012), 60-71
[34] Ali Altaee, Graeme Millar, Guillermo Zaragoza, Adel Sharif, Energy Efficiency of RO and FO-RO system for High Salinity Seawater Treatment, Clean Technology and Environmental Policy, V 19 (2017), 77-91
[35] Ali Altaee, Adel Sharif, A Conceptual NF/RO Arrangement Design in the Pressure Vessel for Seawater Desalination, Journal of Desalination and Water Treatment, 14/January/2014 DOI:10.1080/19443994.2014.890547
[36] N. Pen˜a, S. Gallego, F. del Vigo, S.P. Chesters, Evaluating impact of fouling on reverse osmosis membranes performance, Desalination and Water Treatment, (2012), 1-11, doi: 10.1080/19443994.2012.699509.